crystals

MDPI

Article

Antimonate Removal from Polluted Mining Water by Calcined Layered Double Hydroxides

Elisabetta Dore *, Franco Frau and Rosa Cidu

Department of Chemical and Geological Sciences, University of Cagliari, 09042 Monserrato, Cagliari, Italy
* Correspondence: elisabettadore@yahoo.it

Received: 20 June 2019; Accepted: 1 August 2019; Published: 6 August 2019

Abstract: Calcined layered double hydroxides (LDHs) can be used to remove Sb(V), in the $Sb(OH)_6^-$ form, from aqueous solutions. Sorption batch experiments showed that the mixed MgAlFe oxides, obtained from calcined hydrotalcite-like compound (3HT-cal), removed $Sb(OH)_6^-$ through the formation of a non-LDH brandholzite-like compound, whereas the mixed ZnAl oxides, resulting from calcined zaccagnaite-like compound (2ZC-cal), trapped $Sb(OH)_6^-$ in the interlayer during the formation of a Sb(V)-bearing LDH (the zincalstibite-like compound). The competition effect of coexistent anions on $Sb(OH)_6^-$ removal was $HAsO_4^{2-}$ >> HCO_3^- ≥ SO_4^{2-} for 2ZC-cal and $HAsO_4^{2-}$ >> HCO_3^- >> SO_4^{2-} for 3HT-cal. Considering the importance of assessing the practical use of calcined LDHs, batch experiments were also carried out with a slag drainage affected by serious Sb(V) pollution (Sb = 9900 µg/L) sampled at the abandoned Su Suergiu mine (Sardinia, Italy). Results showed that, due to the complex chemical composition of the slag drainage, dissolved $Sb(OH)_6^-$ was removed by intercalation in the interlayer of carbonate LDHs rather than through the formation of brandholzite-like or zincalstibite-like compounds. Both 2ZC-cal and 3HT-cal efficiently removed very high percentages (up to 90–99%) of Sb(V) from the Su Suergiu mine drainage, and thus can have a potential application for real polluted waters.

Keywords: layered double hydroxides; antimonate uptake; mine water; brandholzite; zincalstibite

1. Introduction

Antimony (Sb) is an element widely present in the environment as a result of both natural processes and anthropogenic sources [1]. Due to its potential risk for human health, the World Health Organization has set the guideline value for drinking water at 20 µg/L of Sb [2], while the European Community has established 5 µg/L [3]. The Sb concentration in uncontaminated freshwater is usually lower than drinking water limits [4,5], however considerable higher concentrations (up to mg/L) can be related to both natural sources and anthropogenic activities [1,4,6–8]. In natural environments, Sb is generally present in the trivalent Sb(III) and pentavalent Sb(V) oxidation states, with the Sb(III) species being ten times more toxic than the Sb(V) ones [9]. In aqueous solution, Sb(III) and Sb(V) prevail, respectively, under reducing and oxidizing conditions as antimonous acid H_3SbO_3 and antimonic acid H_3SbO_4 and their dissociation products, with the $Sb(OH)_6^-$ anion being the most common and stable aqueous species in a wide range of natural pH values [1,9].

Among the techniques suitable for the abatement of Sb concentration in the solution, such as coagulation-flocculation [10], electrochemical methods [11,12] and membrane separation [13,14], the adsorption is considered a low cost and effective method [9]. Several studies reported that metal hydroxides and oxohydroxides (e.g., MnOOH, $Al(OH)_3$, FeOOH) are good Sb removers, however they result more efficient for Sb(III) than Sb(V) under slightly acid to acid conditions [15–18]. Also, nano-TiO_2 electroactive carbon nanotube (CNT) filter and ZrO_2-carbon nanofibers (ZNC) were tested, respectively, for Sb(III) and simultaneous Sb(III) and Sb(V) removal; in particular, it was reported that

the adsorption capacity of Sb(III) is much higher than Sb(V) in ZNC [19,20]. Recent works showed that the acidic conditions are also favorable for the Sb(V) removal from solution by La and Ce-doped magnetic biochars [21,22]. With respect to the other sorbents, layered double hydroxides (LDHs) show the advantage of being able to remove hazardous anions from solution at circumneutral pH, and can therefore be potential removers for $Sb(OH)_6^-$ at the circumneutral pH and oxidizing conditions usually found in the environment [23].

The LDHs are minerals with general formula $[M^{2+}_{1-x}M^{3+}_x(OH)_2](A^{n-})_{x/n}\cdot mH_2O$, where M^{2+} and M^{3+} are respectively bivalent and trivalent metals (Mg^{2+}, Zn^{2+}, Ca^{2+}, Al^{3+}, Fe^{3+}, etc.), A^{n-} are anions (Cl^-, SO_4^{2-}, CO_3^{2-}, etc.) and x is the $M^{3+}/(M^{2+} + M^{3+})$ molar ratio ($0.20 \leq \times \leq 0.33$). The LDHs structure consists of octahedral brucite-like layers positively charged due to the partial substitution of M^{2+} by M^{3+}, stacked along the *c* axis and intercalated with interlayer anions, which neutralize the positive charge, and variable quantity of water molecules [24,25]. The LDHs can successfully remove anionic contaminants from solution through the anion exchange with the interlayer anions, or by trapping anions in the interlayer region during the reconstruction of the layered structure by the rehydration of mixed metal oxides obtained from LDHs calcination (the so called "memory effect") [23,26–29].

Previous authors reported that LDHs with different compositions are potential $Sb(OH)_6^-$ removers: nitrate and chloride bearing Mg-Al LDHs, both untreated and calcined, efficiently remove $Sb(OH)_6^-$ from solution through the formation of a brandholzite-like compound [30,31], and the removal capacity can be improved by doping LDHs with Fe^{2+} [32]; sulfate bearing Zn-Al and Zn-Fe(III) LDHs uptake $Sb(OH)_6^-$ from solution by anion exchange [33,34] and also Fe-Mn LDHs obtained by electro-coagulation process result good removers [35]. Although interest in the use of LDHs for Sb removal from aqueous solutions has increased in recent years, to the best of our knowledge their practical use with real polluted water has not been investigated yet. Therefore, the aim of this study was to assess the $Sb(OH)_6^-$ removal capacity of calcined LDHs from real water affected by serious Sb pollution.

In our previous work we showed that calcined synthetic LDHs with composition like hydrotalcite (with formula $Mg_6(Al_{0.5}Fe_{0.5})_2(CO_3)(OH)_{16}\cdot 4H_2O$) and zaccagnaite (with formula $Zn_4Al_2(CO_3)(OH)_{12}\cdot 3H_2O$) remove $Sb(OH)_6^-$ from solution, respectively, through the formation of a brandholzite-like phase (a non-LDH mineral with general formula $Mg[Sb(OH)_6]_2\cdot 6H_2O$) and a zincalstibite-like compound (an LDH mineral with general formula $Zn_2Al(OH)_6[Sb(OH)_6]$) [36]. In this work we used calcined hydrotalcite-like and zaccagnaite-like compounds to carry out batch experiments with coexistent anions in solution to evaluate their competition effect on $Sb(OH)_6^-$ removal. We successively assessed the practical use of these sorbents with real water by sorption batch experiments performed with the drainage water flowing out from the foundry slag impoundments at the abandoned mine of Su Suergiu (Sardinia, Italy), which is affected by serious Sb pollution [6,37].

2. Materials and Methods

2.1. LDHs Synthesis and Calcination

Synthetic hydrotalcite $Mg_6(Al_{0.5}Fe_{0.5})_2(CO_3)(OH)_{16}\cdot 4H_2O$ and zaccagnaite $Zn_4Al_2(CO_3)(OH)_{12}\cdot 3H_2O$ were prepared with a coprecipitation method at constant pH [36]. Depending on composition, a solution (0.2 M) with the desired metals was prepared by dissolving in ultrapure water (Millipore, Milli-Q©, 18.2 MΩ cm) appropriate amounts of $Mg(NO_3)_2\cdot 6H_2O$, $Al(NO_3)_3\cdot 9H_2O$, $Fe(NO_3)_3\cdot 9H_2O$ and $Zn(NO_3)_2\cdot 6H_2O$. All reagents were of analytical grade (ACS-for analysis, CARLO ERBA Reagents S.r.l., Cornaredo (MI), Italy) and were used without further purification. The so-obtained metal solution was dropped into a reactor containing a Na_2CO_3 solution (0.05 M), under stirring (500 rpm), and the precipitation was induced at constant pH (ranging between 9.5 and 10.5) by adding dropwise a NaOH (0.5 M) solution. After 24 h of aging at 65 °C, the solids were recovered through filtration (30 μm pore size cellulose filter, Whatman Plc, Little Chalfont, Buckinghamshire, UK), washed with deionized water and dried at room temperature. Calcination was performed at 450 °C for 4 h. The M^{2+}/M^{3+} molar ratios of synthetic

hydrotalcite and zaccagnaite, and their calcined products, were close to those of the starting solutions (Table 1).

From now on, synthetic hydrotalcite is termed 3HT and zaccagnaite is 2ZC, the numbers before the labels indicate the M^{2+}/M^{3+} molar ratio; moreover, the suffix -CO_3 will be used for the untreated carbonate LDHs and the suffix -cal for the calcined LDHs.

Table 1. Chemical composition of synthetic untreated carbonate (-CO_3) and calcined (-cal) hydrotalcite-like (3HT) and zaccagnaite-like (2ZC) compounds.

Sample	Zn	Al	M^{2+}/M^{3+}	Sample	Mg	Al	Fe^{3+}	M^{2+}/M^{3+}
	mmol/g	mmol/g	Molar Ratio		mmol/g	mmol/g	mmol/g	Molar Ratio
2ZC-CO_3	6.8	3.2	2.1	3HT-CO_3	7.4	1.3	1.4	2.8
2ZC-cal	9.0	4.1	2.2	3HT-cal	12.5	2.2	2.3	2.8

2.2. Sorption Experiments

2.2.1. Effect of Coexistent Anions

In batch experiments, the coexistent anions were selected taking into account the chemical composition of Su Suergiu mine drainage [6,37]. The experimental solutions were prepared dissolving appropriate amounts of $KSb(OH)_6$ and Na_2SO_4, $NaHCO_3$ or $Na_2HAsO_4{\cdot}7H_2O$ (ACS-for analysis, CARLO ERBA Reagents S.r.l., Cornaredo (MI), Italy) in ultrapure water. To perform the experiments, 0.1 g of 2ZC-cal or 3HT-cal was suspended, for 48 h under stirring, in 400 mL of solution containing equal concentrations (about 1 mmol/L) of dissolved $Sb(OH)_6^-$ and one competitor at a time. Experiments with only dissolved $Sb(OH)_6^-$ without competitors were also carried out to compare the results. Before the addition of the sorbents and during the experiments the pH of solutions was monitored and a portion of solution was withdrawn and acidified with HNO_3 1% *v*/*v* for chemical analysis of Sb, As, S, Mg, Zn, Al and Fe by inductively coupled plasma optical emission spectroscopy (ICP-OES, ARL Fisons 3520, Waltham, MA, USA). At the end of the reaction time the solids were recovered through filtration (0.45 µm pore size polycarbonate filters, Whatman Plc, Little Chalfont, Buckinghamshire, UK), washed with distilled water and dried at room temperature for mineralogical characterization.

2.2.2. Sorption Experiments with Su Suergiu Mine Drainage

The real water for sorption experiments is a slag drainage sampled at the abandoned Su Suergiu mine (Sardinia, Italy), at the sampling point named SU1 (Supplementary Materials Figure S1) as reported by Cidu et al. [37]. The physical and chemical parameters were determined at the sampling site using the sampling protocol described in Cidu et al. [37]. After sampling, the slag drainage (from now on SU1) was stored in HDPE bottles at 4 °C, and batch experiments were carried out, at room temperature (25 °C), less than 24 h after the sampling.

Different amounts of 3HT-cal or 2ZC-cal, equal to 0.1, 0.25, 0.5 and 1 g, were suspended in 400 ml of SU1 under stirring for 24 h. During the experiments the pH of solutions was monitored. At the end of reaction time, the solids were separated from solution through filtration, washed with distilled water and dried at room conditions for mineralogical characterization. The solutions recovered after the experiments were stored in two different aliquots: one aliquot was unacidified for analysis of major ions by ion chromatography (IC, Dionex ICS3000, ThermoFisher SCIENTIFIC, Waltham, MA, USA); a second aliquot was acidified for trace elements analysis (Sb, As, Fe, Zn and Al) by inductively coupled plasma mass spectrometry (ICP-MS, quadrupole, PerkinElmer SCIEX ELAN DRC-e, Waltham, MA, USA) with Rh as internal standard; concentrations of Sb > 1000 µg/L were also determined by ICP-OES.

2.3. Mineralogical Characterization

Mineralogical characterization of synthetic LDHs and their calcined products before and after the experiments was performed by collecting XRD patterns in the 5–80° 2θ angular range on an

automated Panalytical X'pert Pro diffractometer (PANalytical, Almelo, Netherlands), with Ni-filter Cu-Kα_1 radiation (λ = 1.54060 Å), operating at 40 kV and 40 mA, using the X'Celerator detector.

3. Results

3.1. Effect of Coexistent Anions on Sb(V) Removal

3.1.1. Sorptive Competition

The results of competition experiments showed that 2ZC-cal was slightly more effective than 3HT-cal (Figure 1). At the end of the experiments without competitors, 2ZC-cal removed 85% of $Sb(OH)_6^-$ whereas 3HT-cal reached 72%. The coexistence of SO_4^{2-} and HCO_3^- slightly affected the $Sb(OH)_6^-$ uptake by 2ZC-cal, whereas in the experiments with 3HT-cal, the percentage of $Sb(OH)_6^-$ removed did not vary significantly in the presence of SO_4^{2-} but decreased up to 50% with coexistent HCO_3^- (Figure 1, Tables 2 and 3).

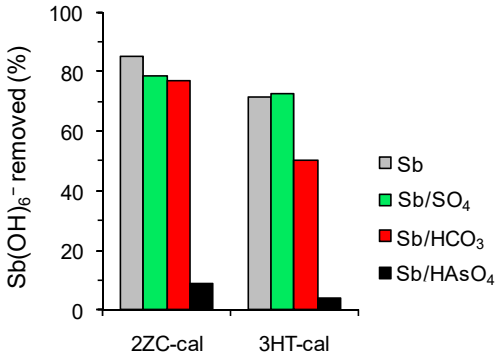

Figure 1. Percentage of $Sb(OH)_6^-$ removed from solution by 2ZC-cal and 3HT-cal at the end of the experiments without competitors (Sb) and with HCO_3^- (Sb/HCO_3), SO_4^{2-} (Sb/SO_4) or $HAsO_4^{2-}$ (Sb/$HAsO_4$) as coexistent anions.

The $HAsO_4^{2-}$ anion was the strongest competitor in the experiments with both 2ZC-cal and 3HT-cal, with percentages of $Sb(OH)_6^-$ removed lower than 10%. Moreover, the $HAsO_4^{2-}$ concentration at the end of the experiment with 3HT-cal markedly decreased by about 60% (Table 3), showing a strong affinity of $HAsO_4^{2-}$ for the interlayer region of 3HT.

Table 2. Solution pH values and dissolved ions determined before and at the end of the sorption experiments performed with 2ZC-cal without competitors (Sb), and with coexistent HCO_3^- (Sb/HCO_3), SO_4^{2-} (Sb/SO_4) or $HAsO_4^{2-}$ (Sb/$HAsO_4$). (A^{n-} = HCO_3^-, SO_4^{2-} or $HAsO_4^{2-}$; na = not analyzed; dl = detection limit; dl_{Zn} = 0.2 µmol/L; dl_{Al} = 7 µmol/L).

Sample	Experiment	Time	pH	$Sb(OH)_6^-$	$Sb(OH)_6^-$ removed	A^{n-}	A^{n-} removed	Zn	Al
		h		mmol/L	%	mmol/L	%	mmol/L	
2ZC-cal	Sb	0	5.1	1.02				0	0
		48	8.5	0.15	85			<dl	<dl
	Sb/HCO_3	0	8.2	1.03		1.09		0	0
		48	8.7	0.24	77	na	na	<dl	<dl
	Sb/SO_4	0	5.2	1.01		1.08		0	0
		48	9.5	0.22	79	1.04	4	<dl	<dl
	Sb/$HAsO_4$	0	8.6	1.02		1.03		0	0
		48	8.1	0.93	8.6	0.87	16	0.02	<dl

The effect of coexistent anions on $Sb(OH)_6^-$ uptake resulted to be $HAsO_4^{2-}$ >> HCO_3^- ≥ SO_4^{2-} for 2ZC-cal and, in partial agreement with previous work [30], $HAsO_4^{2-}$ >> HCO_3^- >> SO_4^{2-} for 3HT-cal.

At the end of the experiments with 3HT-cal, slight concentrations of Mg were determined, whereas the concentrations of Al and Fe were always below the corresponding detection limits (Table 3).

Table 3. Solution pH values and dissolved ions determined before and at the end of the sorption experiments performed with 3HT-cal without competitors (Sb), and with coexistent HCO_3^- (Sb/HCO_3), SO_4^{2-} (Sb/SO_4) or $HAsO_4^{2-}$ (Sb/$HAsO_4$). (A^{n-} = HCO_3^-, SO_4^{2-} or $HAsO_4^{2-}$; na = not analyzed; dl = detection limit; dl_{Al} = 7 µmol/L; dl_{Fe} = 1 µmol/L).

Sample	Experiment	Time	pH	$Sb(OH)_6^-$	$Sb(OH)_6^-$ removed	A^{n-}	A^{n-} removed	Mg	Al	Fe
				mmol/L	%	mmol/L	%	mmol/L		
3HT-cal	Sb	0	5.2	1.03				0	0	0
		48	9.3	0.29	72			0.20	<dl	<dl
	Sb/HCO_3	0	8.3	1.02		1.05		0	0	0
		48	9.5	0.51	50	na	na	0.22	<dl	<dl
	Sb/SO_4	0	5.1	1.03		1.08		0	0	0
		48	9.1	0.28	73	1.06	2	0.33	<dl	<dl
	$Sb/HAsO_4$	0	8.6	1.03		1.02		0	0	0
		48	9.8	0.99	3.7	0.43	57	0.19	<dl	<dl

3.1.2. Kinetics

In the experiments with both 2ZC-cal and 3HT-cal the solution pH values increased sharply (up to about 11) after the addition of sorbents (Figure 2a,b), and decreased after 48 h in the range of 8.1–9.8 (Tables 2 and 3; Figure 2a,b). Most of the $Sb(OH)_6^-$ was removed within the first six hours (Figure 2c,d) indicating that $Sb(OH)_6^-$ uptake occurred mainly during the reconstruction of the lamellar structure of LDHs [36] as schematized in reaction (1):

$$M^{2+}_{1-x}M^{3+}_{x}(OH)_2\,(CO_3)_{\frac{x}{2}} \overset{calcination}{\rightarrow} M^{2+}_{1-x}M^{3+}_{x}O_{1+(\frac{x}{2})} + xSb(OH)^-_6 \overset{reconstruction}{\rightarrow} M^{2+}_{1-x}M^{3+}_{x}(OH)_2(Sb(OH)_6)_x + xOH^- \quad (1)$$

The $Sb(OH)_6^-$ removal as a function of time was studied through the pseudo-first order [38] and the pseudo-second order kinetic models [39].

The $Sb(OH)_6^-$ sorption capacity has been calculated through the Formula (2):

$$q_t = (C_0 - C_t) \cdot V/W \quad (2)$$

where the sorption capacity (q_t) is the amount of $Sb(OH)_6^-$ sorbed per unit of sorbent (mmol/g) at the reaction time t (h), C_0 and C_t are the $Sb(OH)_6^-$ concentrations in solution (mmol/L) before the addition of the sorbent and at the reaction time t, V is the volume of solution (L) and W the weight of sorbent (g).

The pseudo-first order and the pseudo-second order equations are expressed as follows:

$$pseudo-first\ order\ kinetic\ model \qquad k_1 = \frac{2.303}{t}\cdot log\frac{q_e}{q_e - q_t} \quad (3)$$

$$pseudo-second\ order\ kinetic\ model \qquad k_2 = \frac{1}{t}\cdot\frac{q_t}{q_e(q_e - q_t)} \quad (4)$$

where q_e is the $Sb(OH)_6^-$ sorption capacity at equilibrium (mmol/g), k_1 (1/h) and k_2 (g/mmol h) are the rate constant of sorption. These equations expressed in the linear form result as follows:

$$pseudo - first\ order\ kinetic\ model \qquad \frac{dq_t}{dt} = k_1\,(q_e - q_t) \tag{5}$$

$$pseudo - second\ order\ kinetic\ model \qquad \frac{dq_t}{dt} = k_2\,(q_e - q_t)^2 \tag{6}$$

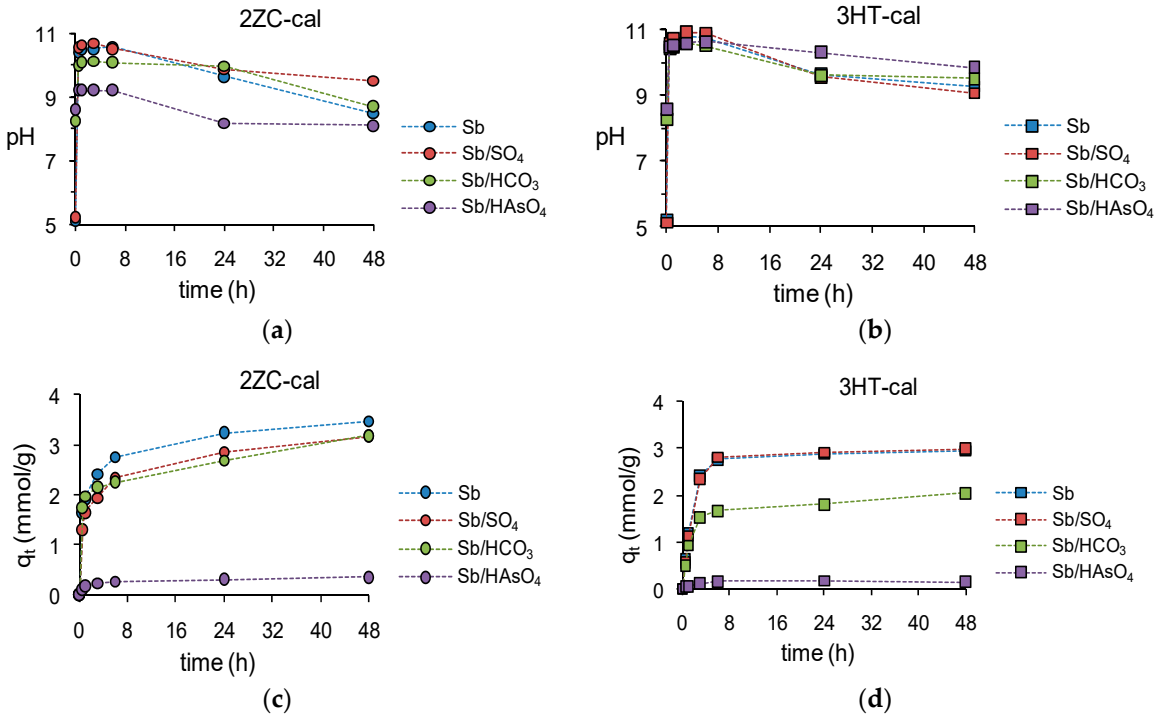

Figure 2. The solution pH values determined as a function of time during the sorption experiments without competitors and with coexistent anions performed with (**a**) 2ZC-cal and (**b**) 3HT-cal. The $Sb(OH)_6^-$ sorption capacity (q_t) as a function of time in the experiments performed with (**c**) 2ZC-cal and (**d**) 3HT-cal without competitors and with coexistent anions.

To verify the applicability of kinetic models at the sorption system, the experimental data were plotted as $\log(q_e - q_t)$ vs. time for the pseudo-first order (Supplementary Material Figure S2) and t/q_t vs. time (Supplementary Material Figure S3) for the pseudo-second order kinetic model. If the plots give a linear correlation, then the theoretical sorption capacity at equilibrium and the rate constants can be calculated from the slope and the intercept of the straight lines. The good fit of the data, the r^2 values close to the unit and the good agreement between the experimental sorption capacity at equilibrium (q_e) and the theoretical sorption capacity (q_{calc}) indicated that the sorption system is better described by the pseudo-second order kinetic model (Table 4), suggesting that the $Sb(OH)_6^-$ uptake by both 2ZC-cal and 3HT-cal might principally occur by chemisorption.

Table 4. The $Sb(OH)_6^-$ sorption capacity of 2ZC-cal and 3HT-cal determined at equilibrium from the experimental data (q_e) and calculated from the kinetic models (q_{calc}).

Sample	Experiment		Pseudo-First Order Kinetic Model			Pseudo-Second Order Kinetic Model		
		q_e mmol/g	q_{calc} mmol/g	k_1 1/h	r^2	q_{calc} mmol/g	k_2 g/mmol h	r^2
2ZC-cal	Sb	3.47	1.86	0.093	0.848	3.52	0.235	0.999
	Sb/HCO_3	3.18	1.59	0.052	0.631	3.19	0.196	0.992
	Sb/SO_4	3.17	1.86	0.080	0.856	3.23	0.186	0.997
	$Sb/HAsO_4$	0.35	4.78	0.068	0.754	0.36	1.568	0.992
3HT-cal	Sb	2.94	1.51	0.143	0.761	3.02	0.272	0.999
	Sb/HCO_3	2.04	1.13	0.074	0.641	2.07	0.303	0.997
	Sb/SO_4	2.99	1.58	0.137	0.738	3.08	0.231	0.999
	$Sb/HAsO_4$	0.15				0.16	12.9	0.995

3.1.3. Characterization of Sorbents

The XRD pattern of 2ZC-CO_3 (Figure 3a) showed the characteristic basal reflections (003) and (006) attributable to a zaccagnaite-like compound [40].

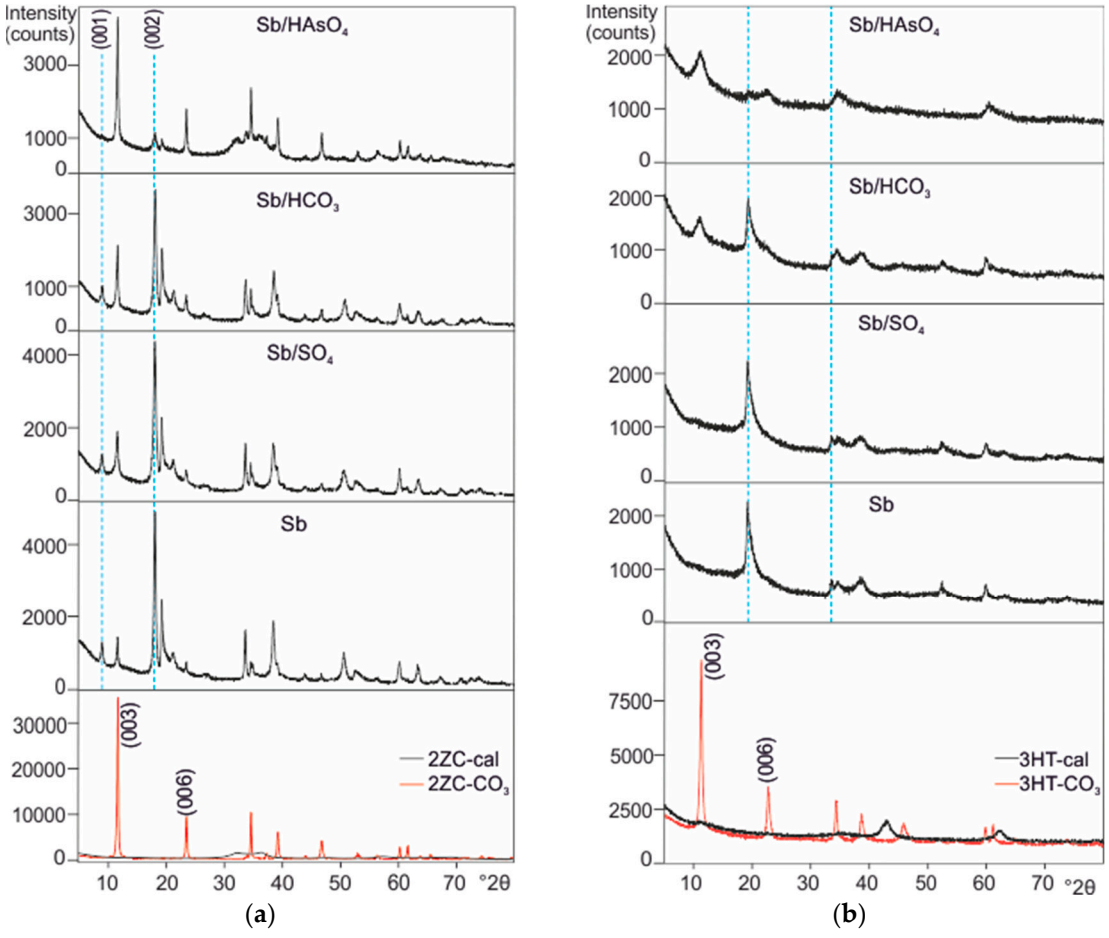

Figure 3. XRD patterns of (**a**) 2ZC-CO_3 and its calcined product 2ZC-cal and of (**b**) 3HT-CO_3 and its calcined product 3HT-cal, and XRD patterns of sorbents recovered after the sorption experiment without competitors (Sb), and with coexistent SO_4^{2-} (Sb/SO_4), HCO_3^- (Sb/HCO_3) or $HAsO_4^{2-}$ ($Sb/HAsO_4$). The blue dashed lines indicate the peaks of the (**a**) zincalstibite-like and (**b**) brandholzite-like compounds formed after the sorption experiments.

After calcination, in the XRD pattern of 2ZC-cal, the absence of LDH basal reflections and the presence of broad peaks at 32.1° and 36.4° 2θ, ascribable to ZnO, indicated the collapse of the lamellar LDH structure and the formation of a disordered ZnO, with Al probably dispersed in its structure [41]. Peaks of undesired phases were not detected. The XRD patterns of solids recovered after the sorption experiments showed two different LDH phases: the peaks at angular position 11.6° and 23.5° 2θ corresponded to the basal reflections (003) and (006) of 2ZC-CO_3; instead, the peaks at 5° and 18° 2θ were attributable, respectively, to the (001) and (002) reflections of a zincalstibite-like compound [36,42].

The characteristic hydrotalcite-like compound basal reflections (003) and (006), visible in the XRD patterns of 3HT-CO_3 (Figure 3b), were no longer detectable in the calcined phase (3HT-cal) which showed peaks at about 42° and 62° 2θ ascribable to a disordered MgO with the trivalent metals Fe and Al probably dispersed in its structure [26]. After the sorption experiments, the solids showed the characteristic peak of a brandholzite-like compound at 19.2° 2θ and a further brandholzite peak at 33.6° 2θ [36,43], except for the experiment with coexistent $HAsO_4^{2-}$ where the characteristic brandholzite peak was barely visible and additional peaks at low angle compatible with the basal reflections of 3HT-CO_3 were clearly recognizable.

3.2. Sorption Experiments with Su Suergiu Mine Drainage (SU1)

3.2.1. Solutions

For convenience in this section the concentrations of ions in solution will be expressed as mg/L and μg/L.

The results of the chemical analysis of SU1 slag drainage showed a Ca-SO_4 dominant chemical composition and high concentrations of Sb (9900 μg/L) and arsenic (As = 3390 μg/L) (Table 5).

Table 5. The pH values, electrical conductivity (EC) and chemical composition of SU1 slag drainage before (SU1 column) and after the sorption experiments performed with different amounts (0.1, 0.25, 0.5, 1g) of 2ZC-cal and 3HT-cal (SU1 + 2ZC-cal and SU1 + 3HT-cal columns).

			SU1 + 2ZC-cal				SU1 + 3HT-cal			
		SU1	Weight of Sorbent (g)				Weight of Sorbent (g)			
			0.1	0.25	0.5	1	0.1	0.25	0.5	1
EC	mS/cm	2.40	2.33	2.24	2.14	2.04	2.24	2.12	1.99	1.75
pH		8.2	8.1	8.1	8.0	7.9	8.4	9.2	9.4	9.7
SO_4	mg/L	1000	1080	1050	1000	960	1070	1050	960	770
HCO_3	mg/L	485	252	169	125	80	127	48	29	18
Cl	mg/L	59	64	65	63	63	64	64	63	63
NO_3	mg/L	0.6	4.4	0.7	1.3	0.6	1.4	1.9	3.5	6.3
F	mg/L	1.7	1.6	1.1	0.5	0.3	0.8	0.4	0.1	0.1
Ca	mg/L	362	278	264	234	244	131	68	80	129
Mg	mg/L	63	62	56	45	25	120	140	109	59
Na	mg/L	166	168	161	167	163	166	166	166	162
K	mg/L	4.7	4.4	4.4	4.8	4.3	4.7	4.6	4.8	4.6
Zn	μg/L	30	1490	174	260	242	<20	<20	<20	<20
Al	μg/L	<30	78	105	67	<30	700	<30	<30	<30
Fe	μg/L	<20	<20	<20	<20	<20	<20	<20	<20	<20
Sb	μg/L	9900	6190	78	34	20	9830	170	430	1000
As	μg/L	3390	92	35	8.3	4.5	150	25	6.5	<0.5

The high value of EC (electrical conductivity) is related to the high contents of Ca^{2+} and SO_4^{2-}, with SO_4^{2-} mainly deriving from the oxidation of sulfides; moreover, the high concentration of HCO_3^- avoids the decrease of pH, which resulted in slightly alkaline values (Table 5). The high concentration of both Sb and As is the consequence of the water interaction with the foundry slags [6,37]. It has been reported that in the Su Suergiu mine water, the Sb(III), when detected, results <2% of total dissolved

Sb (water fraction < 0.45 μm) and that all the Sb(V) occurs as $Sb(OH)_6^-$ [6,44]. The concentration of Sb(III) determined in the SU1 sampled for sorption experiments with 3HT-cal and 2ZC-cal resulted to be 147 μg/L, therefore, in the present work, the $Sb(OH)_6^-$ is considered the only Sb form involved in the Sb removal processes. Excluding the experiments performed with 0.1 g of sorbents, at the end of reaction time up to 90–99% of Sb was removed from the solution, with 2ZC-cal slightly more effective than 3HT-cal (Figure 4a), whereas As was effectively removed in all experiments (Figure 4b). In almost all experiments, the Sb and As concentrations decreased close to, or below, the limits established for drinking water (Figure 4c,d).

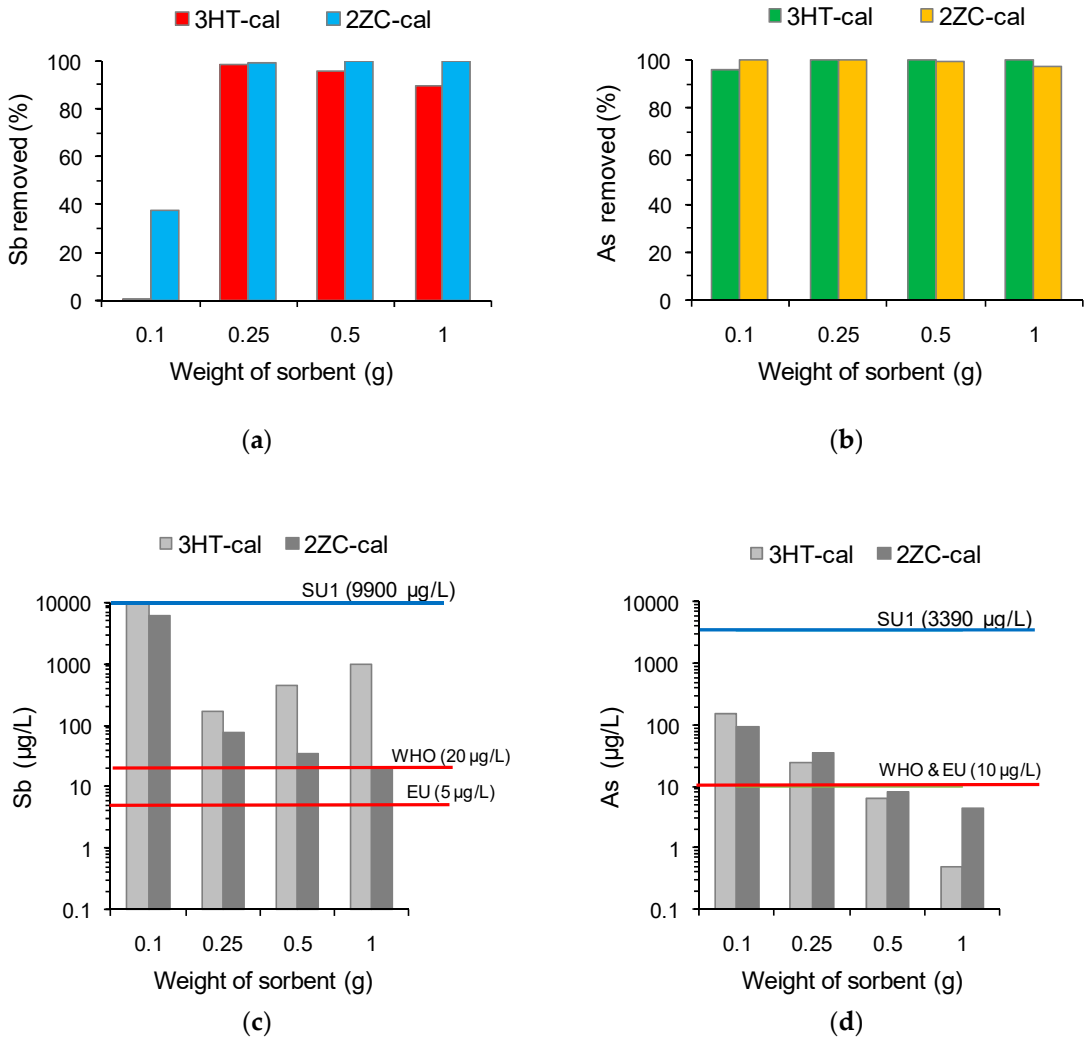

Figure 4. Results of batch sorption experiments performed with 3HT-cal and 2ZC-cal with the Su Suergiu mine drainage (SU1). Percentages of (**a**) Sb and (**b**) As removed at the end of the sorption experiments, and concentrations of residual (**c**) Sb and (**d**) As in solution at the end of the experiments for different amounts of the sorbent. In the plots (**c**) and (**d**) the blue lines indicate the starting Sb or As concentrations; the red lines indicate the limits of Sb and As set for drinking water by the World Health Organization (WHO) [2] and the European Community (EU) [3].

3.2.2. Sorbents

The XRD patterns of solids recovered after all experiments showed peaks at low angles compatible with the carbonate bearing LDHs, indicating the reconstruction of the typical lamellar LDH structure (Figures 5 and 6). In the range of pH values of the experiments, Sb and As prevail, respectively, as $Sb(OH)_6^-$ and $HAsO_4^{2-}$, but peaks attributable to a brandholzite-like compound were not visible in the solids recovered after the experiments performed with 3HT-cal (Figure 5), and only after the

experiment with 0.1 g of 2ZC-cal the characteristic peak of a zincalstibite-like compound was clearly recognizable (Figure 6). Therefore, as a consequence of the complexity of the chemical composition of SU1, the $Sb(OH)_6^-$ removal did not occur through the formation of $Sb(OH)_6^-$ bearing phases, but rather, it is reasonable to suppose that $Sb(OH)_6^-$ was incorporated in the interlayer region together with other anions, i.e., CO_3^{2-} and $HAsO_4^{2-}$. It is also noticeable that all samples contained additional well defined peaks at about 30° 2θ ascribable to calcite (Figures 5 and 6), and after the experiment with 0.1 g of 2ZC-cal, the peaks attributable to monohydrocalcite were also present (Figure 6).

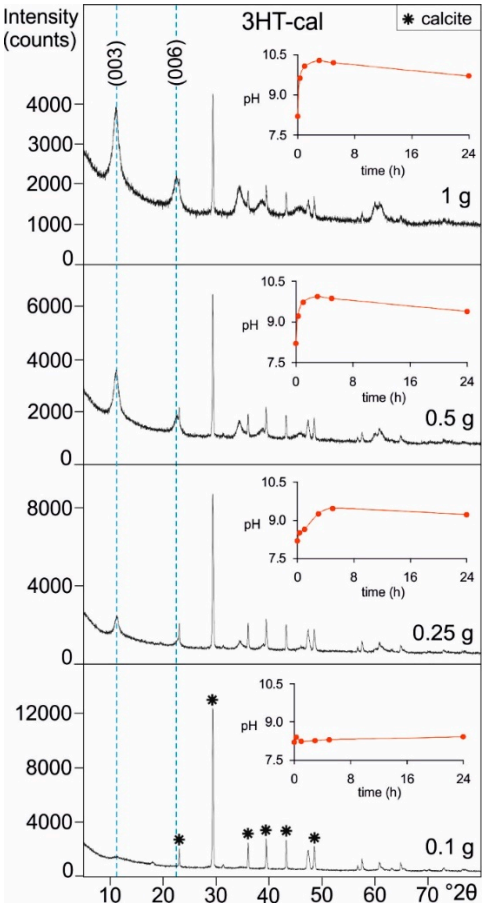

Figure 5. XRD patterns of 3HT-cal recovered after the sorption experiments with the slag drainage SU1 performed with different amounts of 3HT-cal (0.1, 0.25, 0.5, 1 g). On the upper right side of each XRD pattern the pH of solution as a function of time during each experiment is reported. The blue dashed lines indicate the basal reflection of layered double hydroxides (LDHs) formed after the sorption experiments.

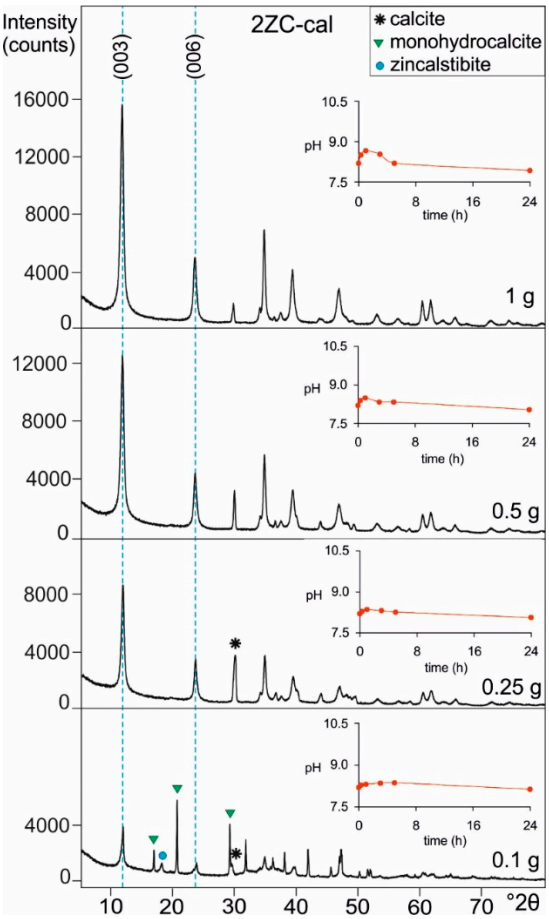

Figure 6. XRD patterns of 2ZC-cal recovered after the sorption experiments with the slag drainage SU1 performed with different amounts of 2ZC-cal (0.1, 0.25, 0.5, 1 g). On the upper right side of each XRD pattern the pH of solution as a function of time during each experiment is reported. The blue dashed lines indicate the basal reflection of LDHs formed after the sorption experiments.

4. Discussion

4.1. Effect of Coexistent Anions

The results of mineralogical characterizations and chemical analysis, in agreement with previous works, showed that 2ZC-cal removed $Sb(OH)_6^-$ from solution through the reconstruction of a zincalstibite-like compound [36], and the 3HT-cal removed $Sb(OH)_6^-$ through the formation of a low ordered brandholzite-like compound [30,36]. The zincalstibite is an $Sb(OH)_6^-$ bearing LDH (with general formula $Zn_2Al(OH)_6[Sb(OH)_6]$ [25,42], whereas the brandholzite is a non-LDH phase with general formula $Mg[Sb(OH)_6]_2{\cdot}6H_2O$, whose the layered structure is characterized by the presence of two layers, $\{[Sb(OH)_6]_9\}^{9-}$ and $\{[Sb(OH)_6]_3[Mg(H_2O)_6]_6\}^{9+}$, alternatively stacked along the *c* axis [43].

In agreement with the results of chemical analysis, the diffraction peaks of the $Sb(OH)_6^-$ bearing phases were more intense and well defined in the XRD patterns of solids recovered after the experiments wherein the greatest amounts of $Sb(OH)_6^-$ were removed from solution. In the experiments performed with 3HT-cal and HCO_3^- and $HAsO_4^{2-}$ as coexistent anions, the decrease in $Sb(OH)_6^-$ removal was linked to the appearance of the (003) and (006) basal reflections of LDHs (Figure 3b). In particular, in the experiment with coexistent HCO_3^- the competition effect was improved by the increase of solution pH values, up to 10.6 (Figure 2b), that favors the prevalence of CO_3^{2-} in solution that has a high affinity for the LDH interlayer [23,30]. Also $HAsO_4^{2-}$ has a high affinity for hydrotalcite-like compounds [27,45], but previous authors have observed that the removal capacity of calcined MgAl-LDHs is higher for $Sb(OH)_6^-$ than for $HAsO_4^{2-}$, suggesting that the uptake of $Sb(OH)_6^-$ through the selective

crystallization of a brandholzite-like compound is more favorable than the sequestration from solution by the intercalation in the interlayer [46]. The results of our work showed that, when coexisting in solution, $HAsO_4^{2-}$ strongly competes with $Sb(OH)_6^-$ and is preferentially removed, probably due to its higher specific ionic charge.

The low amounts of Mg determined at the end of experiments with 3HT-cal indicated a slight dissolution of sorbent (6–15%) (Table 3). Because the concentrations of dissolved Fe and Al were always below the corresponding detection limits and no Al and/or Fe secondary phases were observed in the XRD patterns of solids recovered at the end of experiments (Figure 3b), the low amount of Al and Fe released in the solution might precipitate as amorphous solids. The Fe and Al of undissolved phase that removed the $Sb(OH)_6^-$ through the formation of brandholzite-like compound, probably remained in undetermined sites of the low ordered brandholzite structure.

The XRD pattern of the experiment performed with 2ZC-cal and $HAsO_4^{2-}$ as coexistent anion showed well defined basal reflections compatible with the original 2ZC-CO_3 LDH, while the characteristic zincalstibite-like compound peaks were scarcely visible (Figure 3a). Moreover, two broad undefined humps in the angular ranges 30–33° and 35–37° 2θ indicated that, at the end of the experiment, part of the 2ZC-cal did not react and explained the low $Sb(OH)_6^-$ removal that, unlike the experiment performed with 3HT-cal, cannot be attributable to the preferential uptake of $HAsO_4^{2-}$ (Table 2). Previous authors reported the high affinity of As(V) for sulfate bearing ZnAl-LDHs [47,48] but, at the best of our knowledge, experiments on the As(V) removal by calcined ZnAl-LDHs is lacking and needs further study.

4.2. Sorption Experiments with Su Suergiu Mine Drainage (SU1)

The results suggested that both 2ZC-cal and 3HT-cal are suitable for the Sb (and also As) removal from SU1; however, to assess their practical use, the overall quality of treated water must also be considered. The decrease of EC value after the experiments can be attributable to the decrease of Ca^{2+} and HCO_3^-. The contents of Na^+, K^+ and Cl^- did not vary significantly, instead sensible variations of SO_4^{2-}, NO_3^- and F^- were observed in a few cases. The partial dissolution of sorbents explained the irregular increase of dissolved Zn or Mg and Al. The limit of Al in drinking water is established at 0.2 mg/L by both the WHO and EU, whereas the concentration of Zn in drinking water is not regulated by the WHO and EU, but rather the Italian Legislation set 2 mg/L [49]; therefore, the concentration of Al exceeded the limit only in one experiment and the Zn limit was never reached (Table 5).

In the experiment performed with 0.1 g of 3HT-cal the amount of Sb removed was dramatically lower with respect to the other experiments with higher amounts of 3HT-cal. In this case it was possible to observe that the Sb removal did not increase with the weight of 3HT-cal used. The Ca^{2+} and HCO_3^- decreases did not show correlation (Supplementary material Figure S4). In particular, the Ca^{2+} concentration suggested a lower $CaCO_3$ precipitation at the end of experiments with 0.1 and 1 g of 3HT-cal with respect to the other ones. In the first case (i.e., 0.1 g of 3HT-cal) the $CaCO_3$ precipitation should be limited by the low increase of pH (8.2–8.4), while in the experiment with 1 g of 3HT-cal, where the pH values increase up to 10.3 (Figure 5) and CO_3^{2-} prevails in solution, the $CaCO_3$ precipitation should be hindered by the uptake of CO_3^{2-} in the interlayer during the 3HT-cal rehydration (Figure 5). This could also explain the low Sb removal in spite of the high amount of 3HT-cal. In fact, at high pH the Sb uptake was hindered by CO_3^{2-} that strongly competes for the entry in the interlayer region of the reconstructing lamellar LDH structure. The experiments with 0.5 and 0.25 g of 3HT-cal seemed the best compromise to reach the most favorable conditions for the highest Sb and As removal from 400 mL of SU1.

As observed above, at the end of the experiments with 0.25, 0.5 and 1 g of 2ZC-cal, the amount of Sb removed from solution was markedly higher with respect to 0.1 g of sorbent. Moreover, it is possible to observe that the dissolved concentrations of Sb and As slightly decreased as the amount of 2ZC-cal used increased. The decrease of Ca^{2+} and HCO_3^- observed at the end of the experiments did not show clear correlation (Supplementary material Figure S4). The sequestration of Ca^{2+} is attributable to

the precipitation of calcium carbonates, which can also explain the slight decrease of Mg^{2+} in some cases (Table 5). The slight differences in residual Ca^{2+} concentration indicated the precipitation of nearly equivalent amounts of calcium carbonates in the different experiments (Table 5). Differently, the HCO_3^- concentration decreased as the amount of 2ZC-cal increased because its uptake from the solution occurred by both the precipitation of calcium carbonates and the entry in the interlayer during the LDHs reconstruction (Supplementary material Figure S4). It is possible to note that only in the experiments with 0.5 and 1 g of 2ZC-cal the pH of solution slightly increased after the addition of sorbents (up to 8.7) and successively decreased to 7.9–8.0, whereas in the experiments with 0.1 and 0.25 g, the variation of pH values was negligible and remained in the range of 8.1–8.4 (Figure 6). These limited pH variations among the experiments with 2ZC-cal can explain the precipitation of nearly equivalent amounts of calcium carbonates. The relatively low pH values can also explain the limited precipitation of calcium carbonates, deducible from the concentrations of Ca removed from solution (Supplementary material Figure S4), with respect to that observed in the experiments performed with 3HT-cal. At these pH values around 8, HCO_3^- prevails among the dissolved carbonate species, therefore it is possible that the reconstruction of LDH by rehydration of 2ZC-cal occurred via the intercalation of HCO_3^-, as well as CO_3^{2-}.

In our previous work we performed sorption experiments, carried out with ultrapure water containing only $Sb(OH)_6^-$, to determine the maximum theoretical $Sb(OH)_6^-$ sorption capacity (q_{max}) of 2ZC-cal and 3HT-cal through the Langmuir isotherm [36]. The values of q_{max} were 4.37 mmol/g (i.e., 532 mg/g) for 3HT-cal and 4.54 mmol/g (i.e., 553 mg/g) for 2ZC-cal [36]. In the present work we have observed that the coexistence of other anions in solution can affect the $Sb(OH)_6^-$ removal capacity of sorbents tested. In order to construct the isotherm, being the starting Sb concentration of sorption experiments that of SU1, the solid/liquid ratio has been changed. However, the sorption data did not fit for the calculation of the isotherm because, due to the complexity of the SU1 chemical composition, also other processes, like the precipitation of calcium carbonates, occurred during the interaction between water and calcined LDHs having an effect on the Sb removal.

It is worth mentioning that the LDHs exhibit the possibility of being reused by regeneration, operated through calcination or anion exchange, for consecutive sorption–regeneration–sorption cycles [50–54]. This is a very important characteristic for their practical use in water treatment because it can reduce the amount of post-treatment waste materials. In this regard, as far as we know, there is no data about the regeneration of ZnAl-LDH after Sb(V) adsorption; whereas it has been reported that, because brandholzite is a non-LDH mineral, the brandholzite formation connected with the Sb(V) removal by calcined MgAl-LDHs can negatively affect the MgAl-LDH regeneration capacity [46,55]. In this work we have observed that in the experiments performed with SU1, the Sb(V) removal by 3HT-cal occurred by intercalation in the LDH interlayer. It is reasonable to suppose that this removal mechanism may positively influence the effectiveness of LDHs regeneration. Therefore, further studies should be performed in order to assess the potential use of both 3HT-cal and 2ZC-cal regenerated after Sb(V) removal from real polluted water.

5. Conclusions

In this work the Sb(V) (in the $Sb(OH)_6^-$ form) removal capacity of calcined hydrotalcite-like (3HT-cal) and zaccagnaite-like (2ZC-cal) compounds has been studied in order to assess their potential for the practical use with real Sb(V) polluted water. For this purpose, first the effect of other anions on the $Sb(OH)_6^-$ removal capacity of 2ZC-cal and 3HT-cal were tested through batch sorption experiments with coexistent anions in solution. Successively batch sorption experiments were carried out with the slag drainage (SU1) sampled at the abandoned Su Suergiu mine (Sardinia, Italy) affected by relevant Sb pollution.

In agreement with previous studies, the results of our experiments with coexistent anions showed that 3HT-cal and 2ZC-cal removed $Sb(OH)_6^-$ through the formation of brandholzite-like and zincalstibite-like compounds, respectively. Among the anions tested, the competition effect on

$Sb(OH)_6^-$ removal resulted to be $HAsO_4^{2-}$ >> HCO_3^- ≥ SO_4^{2-} for 2ZC-cal, and $HAsO_4^{2-}$ >> HCO_3^- >> SO_4^{2-} for 3HT-cal.

The results of the sorption experiments showed that both 3HT-cal and 2ZC-cal effectively removed Sb and As from SU1 and, thus, these phases might have potential use for practical application with real polluted water. In the case under study, due the high concentration of carbonate species in SU1, Sb was mainly removed by intercalation in the interlayer of carbonate bearing LDHs rather than by the formation of zincalstibite-like and brandholzite-like compounds, as instead observed in the competition experiments performed with synthetic solutions. The results also indicated that the precipitation of calcium carbonates (i.e., calcite and monohydrocalcite) may favor the Sb removal, subtracting CO_3^{2-} from the solution as a possible strong competitor of Sb for the interlayer region of LDHs. Therefore, especially in the experiments with 3HT-cal, the Sb removal capacity was markedly influenced by the liquid/solid ratio that determines the solution pH, the correlated precipitation of calcium carbonates and the competition effect of carbonate species in solution. The Sb removal by intercalation in the interlayer of carbonate bearing LDHs rather than the formation of antimonate bearing phases may represent an advantage for the LDHs regeneration, therefore further studies should be addressed in that direction.

Supplementary Materials: The following are available online at http://www.mdpi.com/2073-4352/9/8/410/s1, Figure S1: The abandoned mine area of Su Suergiu (Cidu et al [34], modified); Figure S2: The linear kinetic plots of the pseudo-first order rate equation of $Sb(OH)_6^-$ sorption experiments performed without competitors and with coexistent anions performed with (**a**) 2ZC-cal and (**b**) 3HT-cal; Figure S3: The linear kinetic plots of the pseudo-second order rate equation of $Sb(OH)_6^-$ sorption experiments without competitors and with coexistent SO_4^{2-} and HCO_3^- performed with (**a**) 2ZC-cal and (**b**) 3HT-cal, and (**c**) performed with $HAsO_4^{2-}$; Figure S4: (**a**) Plot of Ca removed vs HCO_3 removed, and concentration of (**b**) Ca and (**c**) HCO_3 removed at the end of the experiments performed with 3HT-cal or 2ZC-cal and SU1. The horizontal green lines in the plots (**b**) and (**c**) indicate the starting concentrations of Ca or HCO_3, respectively.

Author Contributions: Conceptualization, E.D., F.F. and R.C.; Data curation, E.D.; Formal analysis, E.D.; Funding acquisition, F.F. and R.C.; Investigation, E.D.; Methodology, E.D.; Supervision, F.F. and R.C.; Validation, F.F. and R.C.; Writing—original draft, E.D.; Writing—review and editing, E.D., F.F. and R.C.

Funding: Authors thank the financial support from the Ministero Università Ricerca Scientifica Tecnologica through the research projects PRIN 2009 (Coordinator R. Cidu) and PRIN 2010–2011 (Coordinator P. Lattanzi).

Acknowledgments: Authors thank the Dott.ssa Paola Meloni and Dott.ssa Ombretta Cocco of "Research and Didactic Laboratory for the Conservation of the artistic heritage of the Monumental Cemetery of Bonaria" (Department of Mechanical, Chemical and Materials Engineering (DIMCM), University of Cagliari) for the assistance with the XRD measurements.

Conflicts of Interest: The authors declare no conflict of interest.

References

1. Filella, M.; Belzile, N.; Chen, Y.W. Antimony in the environment: A review focused on natural waters I. Occurrence. *Earth Sci. Rev.* **2002**, *57*, 125–176. [CrossRef]
2. WHO. *World Health Organization: Guidelines for Drinking Water Quality*, 4th ed.; WHO: Geneva, Switzerland, 2011.
3. Council of the European Union. Council Directive 98/83/EC of 3 November 1998 on the quality of water intended for human consumption. *Off. J. Eur. Communities* **1998**, *330*, 35–54.
4. Filella, M.; Belzile, N.; Chen, Y.W.; Quentel, F. Antimony in the environment: A review focused on natural waters II. Relevant solution chemistry. *Earth Sci. Rev.* **2002**, *59*, 265–285. [CrossRef]
5. Reimann, C.; Matschullat, J.; Birke, M.; Salminen, R. Antimony in the environment: Lessons from geochemical mapping. *Appl. Geochem.* **2010**, *25*, 175–198. [CrossRef]
6. Cidu, R.; Dore, E.; Biddau, R.; Nordstrom, D.K. Fate of Antimony and Arsenic in Contaminated Waters at the Abandoned Su Suergiu Mine (Sardinia, Italy). *Mine Water Environ.* **2018**, *37*, 151–165. [CrossRef]
7. He, M.; Wang, X.; Wu, F.; Fu, Z. Antimony pollution in China. *Sci. Total. Environ.* **2012**, *421*, 41–50. [CrossRef]
8. Okkenhaug, G.; Gebhardt, K.H.G.; Amstaetter, K.; Bue, H.L.; Herzel, H.; Mariussen, E.; Almas, Å.R.; Cornelissen, G.; Breedveld, G.; Rasmussen, G.; et al. Antimony (Sb) and lead (Pb) in contaminated shooting range soils: Sb and Pb mobility and immobilization by iron based sorbents, a field study. *J. Hazard. Mater.* **2016**, *307*, 336–343. [CrossRef] [PubMed]

9. Li, J.; Zheng, B.; He, Y.; Zhou, Y.; Chen, X.; Ruan, S.; Yang, Y.; Dai, C.; Tang, L. Antimony contamination, consequences and removal techniques: A review. *Ecotox. Environ. Saf.* **2018**, *156*, 125–134. [CrossRef]
10. Guo, X.; Wu, Z.; He, M. Removal of antimony (V) and antimony (III) from drinking water by coagulation-flocculation-sedimentation (CFS). *Water Res.* **2009**, *43*, 4327–4335. [CrossRef]
11. Bergmann, M.E.H.; Koparal, A.S. Electrochemical antimony removal from accumulator acid: Results from removal trials in laboratory cells. *J. Hazard. Mater.* **2011**, *196*, 59–65. [CrossRef]
12. Zhu, J.; Wu, F.; Pan, X.; Guo, J.; Wen, D. Removal of antimony from antimony mine flotation wastewater by electrocoagulation with aluminum electrodes. *J. Environ. Sci.* **2011**, *23*, 1066–1071. [CrossRef]
13. Ma, B.; Wang, X.; Liu, R.; Jefferson, W.A.; Lan, H.; Liu, H.; Qu, J. Synergistic process using Fe hydrolytic flocs and ultrafiltration membrane for enhanced antimony (V) removal. *J. Membr. Sci.* **2017**, *537*, 93–100. [CrossRef]
14. Saito, T.; Tsuneda, S.; Hirata, A.; Nishiyama, S.; Saito, K.; Saito, K.; Sugita, K.; Uezu, K.; Tamada, M.; Sugo, T. Removal of antimony (III) using polyol-ligand-containing porous hollow-fiber membranes. *Sep. Sci. Technol.* **2010**, *39*, 3011–3022. [CrossRef]
15. Leuz, A.K.; Mönch, H.; Johnson, C.A. Sorption of Sb(III) and Sb(V) to goethite: Influence on Sb(III) oxidation and mobilization. *Environ. Sci. Technol.* **2006**, *40*, 7277–7282. [CrossRef] [PubMed]
16. Rakshit, S.; Sarkar, D.; Punamiya, P.; Datta, R. Antimony sorption at gibbsite-water interface. *Chemosphere* **2011**, *84*, 480–483. [CrossRef] [PubMed]
17. Thanabalasingam, P.; Pickering, W.F. Specific sorption of antimony (III) by the hydrous oxides of Mn, Fe and Al. *Water Air Soil Poll.* **1990**, *49*, 175–185. [CrossRef]
18. Watkins, R.; Weiss, D.; Dubbin, W.; Peel, K.; Coles, B.; Arnold, T. Investigation into the kinetics and thermodynamics of Sb(III) adsorption on goethite (α-FeOOH). *J. Colloid Interf. Sci.* **2006**, *303*, 639–646. [CrossRef]
19. Liu, Y.; Wu, P.; Liu, F.; Li, F.; An, X.; Liu, J.; Wang, Z.; Shen, C.; Sand, W. Electroactive modified carbon nanotube filter for simultaneous detoxification and sequestration of Sb(III). *Environ. Sci. Technol.* **2019**, *53*, 1527–1535. [CrossRef]
20. Luo, J.; Luo, X.; Critteden, J.; Qu, J.; Bai, Y.; Peng, Y.; Li, J. Removal of antimonite (Sb(III)) and antimonate (Sb(V)) from aqueous solution using carbon nanofibers that are decorated with zirconium oxide (ZrO_2). *Environ. Sci. Technol.* **2015**, *49*, 11115–11124. [CrossRef]
21. Wang, L.; Wang, J.; Wang, Z.; He, C.; Lyu, W.; Yan, W.; Yang, L. Enhanced antimonate (Sb(V)) removal from aqueous solution by La-doped magnetic biochars. *Chem. Eng. J.* **2018**, *354*, 623–632. [CrossRef]
22. Wang, L.; Wang, J.; Wang, Z.; Feng, J.; Li, S.; Yan, W. Synthesis of Ce-doped magnetic biochar for effective Sb(V) removal: Performance and mechanism. *Powder Technol.* **2019**, *345*, 501–508. [CrossRef]
23. Goh, K.H.; Lim, T.T.; Dong, Z. Application of layered double hydroxides for removal of oxyanions: A review. *Water Res.* **2008**, *42*, 1343–1368. [CrossRef] [PubMed]
24. Cavani, F.; Trifirò, F.; Vaccari, A. Hydrotalcite-type anionic clays: Preparation, properties and applications. *Catal. Today* **1991**, *11*, 173–301. [CrossRef]
25. Mills, S.J.; Christy, A.G.; Génin, J.-M.R.; Kameda, T.; Colombo, F. Nomenclature of the hydrotalcite supergroup: Natural layered double hydroxides. *Mineral. Mag.* **2012**, *76*, 1289–1336. [CrossRef]
26. Carriazo, D.; del Arco, M.; Martín, C.; Rives, V. A comparative study between chloride and calcined carbonate hydrotalcites as adsorbent for Cr(VI). *Appl. Clay Sci.* **2007**, *37*, 231–239. [CrossRef]
27. Wang, S.L.; Cheng, H.L.; Ming, K.W.; Chuang, Y.H.; Chiang, P.N. Arsenate adsorption by Mg/Al-NO_3 layered double hydroxides with varying the Mg/Al ratio. *Appl. Clay Sci.* **2009**, *43*, 79–85. [CrossRef]
28. You, Y.W.; Vance, G.F.; Zhao, H.T. Selenium adsorption on Mg-Al and Zn-Al layered double hydroxides. *Appl. Clay Sci.* **2001**, *20*, 13–25. [CrossRef]
29. Iftekhar, S.; Küçük, M.E.; Srivastava, V.; Repo, E.; Sillanpää, M. Application of zinc-aluminium layered double hydroxides for adsorptive removal of phosphate and sulfate: Equilibrium, kinetic and thermodynamic. *Chemosphere* **2018**, *209*, 470–479. [CrossRef]
30. Kameda, T.; Honda, M.; Yoshioka, T. Removal of antimonate ions and simultaneous formation of a brandholzite-like compound from magnesium-aluminum oxide. *Sep. Purif. Technol.* **2011**, *80*, 235–239. [CrossRef]

31. Kameda, T.; Nakamura, M.; Yoshioka, T. Removal of antimonate ions from an aqueous solution by anion exchange with magnesium-aluminum layered double hydroxides and the formation of a brandholzite-like structure. *J. Environ. Sci. Heal. A* **2012**, *47*, 1146–1151. [CrossRef]
32. Kameda, T.; Kondo, E.; Yoshioka, T. Equilibrium and kinetics studies on As(V) and Sb(V) removal by Fe^{2+}-doped Mg-Al layered double hydroxides. *J. Environ. Manag.* **2015**, *151*, 303–309. [CrossRef] [PubMed]
33. Ardau, C.; Frau, F.; Lattanzi, P. Antimony removal from aqueous solutions by the use of Zn-Al sulphate Layered Double Hydroxide. *Water Air Soil Poll.* **2016**, *227*, 344. [CrossRef]
34. Lu, H.; Zhu, Z.; Zhang, H.; Zhu, J.; Qiu, Y. Simultaneous removal of arsenate and antimonate in simulated and practical water samples by adsorption onto Zn/Fe layered double hydroxide. *Chem. Eng. J.* **2015**, *276*, 365–375. [CrossRef]
35. Cao, D.; Zeng, H.; Yang, B.; Zhao, X. Mn assisted electrochemical generation of two-dimensional Fe-Mn layered double hydroxides for efficient Sb(V) removal. *J. Hazard. Mater.* **2017**, *336*, 33–40. [CrossRef] [PubMed]
36. Dore, E.; Frau, F. Antimonate uptake by calcined and uncalcined layered double hydroxides: Effect of cationic composition and M^{2+}/M^{3+} molar ratio. *Environ. Sci. Pollut. Res.* **2018**, *25*, 916–929. [CrossRef] [PubMed]
37. Cidu, R.; Biddau, R.; Dore, E.; Vacca, A.; Marini, L. Antimony in the soil-water-plant system at the Su Suergiu abandoned mine (Sardinia, Italy): Strategies to mitigate contamination. *Sci. Total. Environ.* **2014**, *497*, 319–331. [CrossRef] [PubMed]
38. Lagergren, S. About the theory of so-called adsorption of soluble substances. *K. Sven. Vetensk. Handl.* **1898**, *24*, 1–39.
39. Ho, Y.S.; McKay, G. A comparison of chemisorption kinetic models applied to pollutant removal on various sorbents. *Process. Saf. Environ.* **1998**, *76*, 332–340. [CrossRef]
40. Lozano, R.P.; Rossi, C.; La Iglesia, Á.; Matesanz, E. Zaccagnaite-3R, a new Zn-Al polytype from El Soplao cave (Cantabria, Spain). *Am. Minerol.* **2012**, *97*, 513–523. [CrossRef]
41. Zhang, Y.; Li, X. Preparation of Zn-Al CLDH to remove bromate from drinking water. *J. Environ. Eng. Asce* **2014**, *140*, 04014018. [CrossRef]
42. Bonaccorsi, E.; Merlino, S.; Orlandi, P. Zincalstibite, a new mineral, and cualstibite: Crystal chemical and structural relationships. *Am. Minerol.* **2007**, *92*, 198–203. [CrossRef]
43. Friedrich, A.; Wildner, M.; Tillmanns, E.; Merz, P.L. Cristal chemistry of the new mineral brandholzite, $Mg(H_2O)_6[Sb(OH)_6]_2$, and of the synthetic analogues $M^{2+}(H_2O)_6[Sb(OH)_6]_2$ (M^{2+} = Mg, Co). *Am. Minerol.* **2000**, *85*, 593–599. [CrossRef]
44. Cidu, R.; Biddau, R.; Dore, E. Determination of traces of Sb(III) using ASV in Sb-rich water samples affected by mining. *Anal. Chim. Acta* **2015**, *854*, 34–39. [CrossRef] [PubMed]
45. Türk, T.; Alp, I.; Deveci, H. Adsorption of As(V) from water using Mg–Fe-based hydrotalcite (FeHT). *J. Hazard. Mater.* **2009**, *17*, 1665–1670. [CrossRef] [PubMed]
46. Lee, S.H.; Tanaka, M.; Takahashi, Y.; Kim, K.W. Enhanced adsorption of arsenate and antimonate by calcined Mg/Al layered double hydroxide: Investigation of comparative adsorption mechanism by surface characterization. *Chemosphere* **2018**, *211*, 903–911. [CrossRef] [PubMed]
47. Ardau, C.; Frau, F.; Lattanzi, P. New data on arsenic sorption properties of Zn-Al sulphate layered double hydroxides: Influence of competition with other anions. *App. Clay Sci.* **2013**, *80*, 1–9. [CrossRef]
48. Ardau, C.; Frau, F.; Ricci, P.C.; Lattanzi, P. Sulphate-arsenate exchange properties of Zn-Al layered double hydroxides: Preliminary data. *Period. Minerol.* **2011**, *80*, 339–349.
49. GURI. *Decreto Legislativo 3 Aprile 2006, n. 152, Norme in Materia Ambientale*; Gazzetta Ufficiale della Repubblica Italiana: Roma, Italia, 2006. Suppl. ord. n. 96. (In Italian)
50. Bhaumik, A.; Samanta, S.; Mal, N.K. Efficient removal of arsenic from polluted ground water by using a layered double hydroxide exchanger. *Indian J. Chem. A* **2005**, *44*, 1406–1409.
51. Dessalegne, M.; Zewge, F.; Pfenninger, N.; Johnson, C.A.; Diaz, I. Layered double hydroxide and its calcined product for fluoride removal from groundwater of Ethiopian Rift Valley. *Water Air Soil Pollut.* **2016**, *227*, 381. [CrossRef]
52. Dore, E.; Frau, F. Calcined and uncalcined carbonate layered double hydroxides for possible water defluoridation in rural communities of the East African Rift Valley. *J. Water Process. Eng.* **2019**, *31*, 100855. [CrossRef]
53. Kuzawa, K.; Jung, Y.J.; Kiso, Y.; Yamada, T.; Nagai, M.; Lee, T.G. Phosphate removal and recovery with a synthetic hydrotalcite as an adsorbent. *Chemosphere* **2006**, *62*, 45–52. [CrossRef] [PubMed]

54. Lazaridis, N.K.; Pandi, T.A.; Matis, K.A. Chromium(VI) removal from aqueous solutions by Mg–Al–CO_3 hydrotalcite: Sorption–desorption kinetic and equilibrium studies. *Ind. Eng. Chem. Res.* **2004**, *43*, 2209–2215. [CrossRef]
55. Lee, S.H.; Choi, H.; Kim, K.W. Removal of As(V) and Sb(V) in water using magnetic nanoparticle-supported layered double hydroxide nanocomposites. *J. Geochem. Explor.* **2018b**, *184*, 247–254. [CrossRef]